Selection of micro-fabrication techniques on stainless steel sheet for skin friction

Zhang, S.; Zeng, X.; Matthews, D. T A; Igartua, A.; Rodriguez-Vidal, E.; Contreras Fortes, J.; Saenz de Viteri, V.; Pagano, F.; Wadman, B.; Wiklund, E. D.

DOI
10.1007/s40544-016-0115-9

Publication date
2016

Document Version
Final published version

Published in
Friction

Citation (APA)
Zhang, S., Zeng, X., Matthews, D. T. A., Igartua, A., Rodriguez-Vidal, E., Contreras Fortes, J., Saenz de Viteri, V., Pagano, F., Wadman, B., Wiklund, E. D., & van der Heide, E. (2016). Selection of micro-fabrication techniques on stainless steel sheet for skin friction. *Friction*, *4*(2), 89-104. https://doi.org/10.1007/s40544-016-0115-9

Friction **4**(2): 89–104 (2016)
DOI 10.1007/s40544-016-0115-9
ISSN 2223-7690
CN 10-1237/TH

REVIEW ARTICLE

Selection of micro-fabrication techniques on stainless steel sheet for skin friction

S. ZHANG[1,*], X. ZENG[1,2], D. T. A. MATTHEWS[3], A. IGARTUA[4], E. RODRIGUEZ-VIDAL[4], J. CONTRERAS FORTES[5], V. SAENZ DE VITERI[4], F. PAGANO[4], B. WADMAN[6], E. D. WIKLUND[6], E. VAN DER HEIDE[1,7]

[1] *Laboratory for Surface Technology and Tribology, Faculty of Engineering Technology, University of Twente, Drienerlolaan 5, Enschede 7522 NB, the Netherlands*

[2] *Shanghai Advanced Research Institute, Chinese Academy of Sciences, Shanghai 201210, China*

[3] *Tata Steel, Research & Development, Ijmuiden 1970 CA, the Netherlands*

[4] *IK4-Tekniker, C/Ignacio Goenaga 5, Eibar 20600, Spain*

[5] *Acerinox Europa SAU, Los Barrios, Spain*

[6] *Swerea IVF, Argongatan 30, Molndal 43153, Sweden*

[7] *TU Delft, Faculty of Civil Engineering and Geosciences, Stevinweg 1, Delft 2628 CN, the Netherlands*

Received: 06 April 2016 / Revised: 09 May 2016 / Accepted: 18 May 2016

Abstract: This review gives a concise introduction to the state-of-art techniques used for surface texturing, e.g., wet etching, plasma etching, laser surface texturing (LST), 3D printing, etc. In order to fabricate deterministic textures with the desired geometric structures and scales, the innovative texturing technologies are developed and extended. Such texturing technology is an emerging frontier with revolutionary impact in industrial and scientific fields. With the help of the latest fabrication technologies, surface textures are scaling down and more complex deterministic patterns may be fabricated with desired functions, e.g., lotus effect (hydrophobic), gecko feet (adhesive), haptic tactile, etc. The objective of this review is to explore the surface texturing technology and its contributions to the applications.

Keywords: microfabrication; surface texturing

1 Introduction

Surface texturing is a well-known engineering technology for enhancing the tribological properties of mechanical components, i.e., wear resistance and friction reduction, and for creating lubricant reservoirs or pockets, see Refs. [1–7]. The functionality of the engineered surfaces defines specific characteristics of the surface texturing process, such as enhancing the lifetime of bearing components [8], or increasing formability of steel [9]. With the development of new and existing fabrication technologies, surfaces with detailed micro-topography can be fabricated as micro-pits or grooves to effectively improve the tribological properties [10]. As the surface texturing techniques developed and expanded over the years, the functionality of surface topography can be further comprehended and more applications appeared [11–13]. As the result, the textures are scaling-down further and more complex structures can be produced for broader applications, including skin friction and tactility [14, 15].

In the field of tactile perception, a substantial amount of work was conducted to understand how people explore and perceive the textured counter-surface by exploring with the finger pads [16]. Klatzky and Lederman [17] studied the geometric properties of sandpaper-surfaces based on the roughness perception while measuring behavioral and neurophysiological responses. In the work of Skedung et al. [18], finger

* Corresponding author: S. ZHANG.
E-mail: s.zhang@utwente.nl

friction measurements are evaluated to determine the relationship between the coefficient of friction (COF) and surface roughness of a series of printing papers. Furthermore, Skedung et al. [19] investigated the relationship between the perceptual dimensions and the implicated physical dimensions on the micro-structured polydimethylsiloxane (PDMS) samples, and found that people are capable of dynamically detecting surface structures with wavelength of 760 nm and amplitude of 13 nm. From the tribological perspective, the parameters of surface texture including spacing, amplitude and waviness are influential factors in skin tribology. The required levels for a polymeric surface can be seen from Fig. 1. The work of Tomlinson et al. [20] found that adhesion component of friction is the predominant mechanism for samples with shallow ridges of a height lower than 42.5 μm. However, with greater height, the skin penetration to the texture ridges increases the amount of hysteresis friction. Same phenomena are found for the width and size of the ridges.

2 Skin tribology

Skin tribology is a relatively new branch of tribology—the science and technology of interacting surfaces in relative motion—and the human skin is always one of the interacting surfaces. The human skin is a multi-layered living material mainly composed of epidermis, dermis and hypodermis. The stratum corneum, the outmost layer of epidermis, is the shield protecting the entire human body from the surrounding environment. Since it is directly in contact with the counter-body, therefore, it serves an important role in hydration control and in tactile friction. Sensory receptors lay in the layer of dermis which has a role in the tribological response. For the layer of hypodermis, which is the deepest layer of human skin, has the least influence in skin mechanical properties compared to the other layers. Overall, the skin behaves in viscoelastic, non-homogeneous and anistropic manner under load. In addition, many factors including the body site, age, hydration level and perhaps nutritional conditions can affect the tribological behaviour of skin, see the work of Veijgen [21]. The dynamic friction generated between the skin and counter-surface is a tangential force resisting the moving motion. The skin friction is related to the deformation of the bodies in contact and generated in breaking the adhesive bonds between the skin and counter-surface in the micro-contacts. It depends on the factors including the operational conditions, material properties, surface

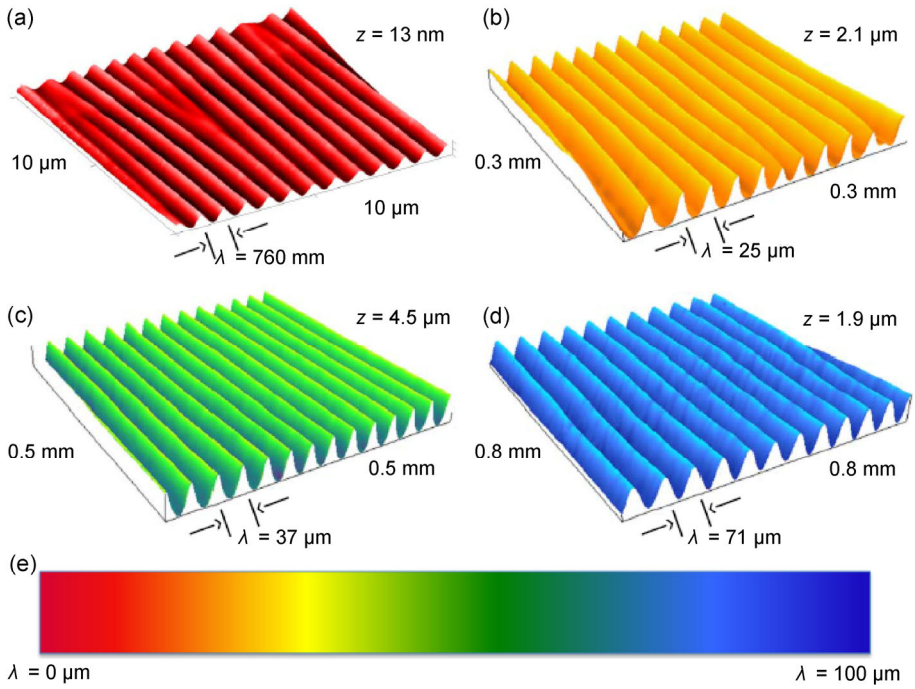

Fig. 1 Wrinkled-patterned polymeric surfaces with textures for touch perception ranging from nanometers to micrometers [19].

structures and environmental conditions (refer to Fig. 2), reflecting the dependence of friction on the tribological system.

In vivo skin friction measurements were carried out by many researchers, and friction generated between the skin and the counter-surface could be categorized based on the results into two main components: deformation component of friction and the adhesion component of friction [22]. The adhesion component of friction plays the dominant role for both dry and humid conditions in sliding contacts between skin and other surfaces [23, 24]. Most experiments are conducted based on skin in dry conditions, because most sliding touches for consumers' products occur in dry conditions. From the mechanical point of view, the real contact area is an important factor in the skin friction, especially the adhesion component of friction. According to the research, skin friction decreases with the reduction of the real contact area [15] just as for other systems where the adhesive component of friction is dominant [25].

$$F_{\mathrm{f,adh}} = \tau A_{\mathrm{real}} \tag{1}$$

where $F_{\mathrm{f,adh}}$ represents the adhesion component of friction; A_{real} is the real contact area; τ is the interfacial shear strength. For the interfacial shear strength τ, it has been found to have a linear function of the average contact pressure ($\overline{p}$)as:

$$\tau = \tau_0 + \alpha \overline{p} \tag{2}$$

where τ_0 is the intrinsic interfacial shear strength; α is the pressure coefficient. After combining Eqs. (1) and (2), the coefficient of friction can be expressed as following:

$$\mu = \frac{F_{\mathrm{f,adh}}}{F_{\mathrm{N}}} = \frac{\tau}{\overline{p}} = \frac{\tau_0 A_{\mathrm{real}}}{F_{\mathrm{N}}} + \alpha \tag{3}$$

The adhesion component of friction is directly related to the real contact area, and the reduction of real contact area is expected to greatly decrease friction. Therefore, the surface texture plays an important role in the tactile friction. With pre-defined deterministic surface texture, the friction generated between the skin and micro-structured counter-surface can be manipulated. Before designing any geometric structures with desired functionality on the stainless steel sheet, the knowledge of basic concepts and feasibility of the micro-fabrication techniques that allow for predefined, deterministic textures, are important. As the spine of texture design, various surface texturing techniques have to be discussed and studied. In the following sections, the core texturing techniques for deterministic textures at the required scale are introduced from retrospective to the state-of-art, and finally the best suitable fabrication technique will be selected to produce the designed deterministic micro-structures on stainless steel sheet samples.

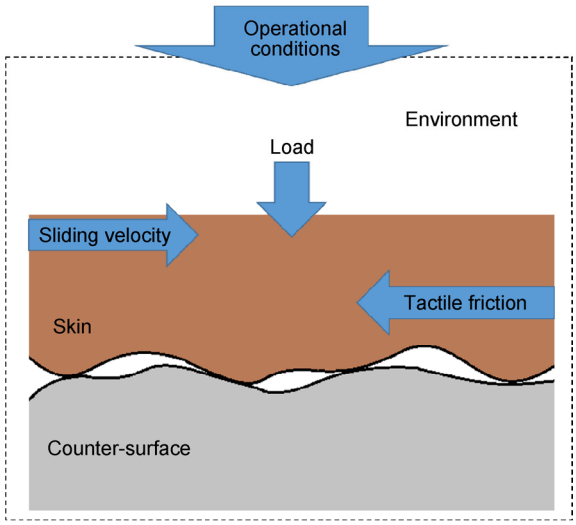

Fig. 2 Tribological system of skin friction.

3 Micro-fabrication techniques

3.1 Micro-casting

Casting is one of the key fabrication techniques for manufacturing and generally known as lost-mold technique by using a textured mold with materials melt into it [26, 27]. First, the mold texture needs to be produced by other micro-fabrication techniques including laser surface texturing, 3D printing and other various micro-fabrication techniques in order to create the deterministic pattern. In general, the plastic or wax pattern is produced and embedded in a ceramic slip. The dried mold will be filled with melt materials, and the pattern will be lost due to melting and burning and transfer the texture to the filling materials. After solidification, the mold is mechanically removed without damaging the cast surface. Depending

on the casting and mold materials, additional chemical cleaning processes may be applied as an extra step.

This technique has been successfully applied for micro-fabricating miniaturized devices for mechanical engineering and bio-mimic duplication [28, 29]. For example of fabricating complicated metal micro-components, the group of Li et al. successfully produced a three-dimensional Zn-Al4 alloy microgear including one gear panel and two gear shafts by using metal mold micro-scale precision casting method [30]. Another study uses micro-casting technique to replicate the surface microstructures that contributes to the lotus leaf effect—superhydrophobicity [31]. The lotus surface is directly replicated via a two-stage (negative-positive) direct micro-casting method using three different materials: vinyl polysiloxane (VPS), polydimethylsiloxane (PDMS) and polymethylmethacrylate (PMMA). During the fabrication process, a negative template with the microstructures of lotus leaf was made first by pouring VPS directly onto a section of the lotus lead. After peeled off the lotus leaf, a positive template was created by pouring PDMS onto the cured negative template (refer to Fig. 3). The same process was used to fabricate PDMS-PMMA replicates. Under the pattern examination, VPS-PMMA and PDMS-PMMA replicates display shorter peak heights and larger base widths with contact angles of 132.1° and 129.2° respectively.

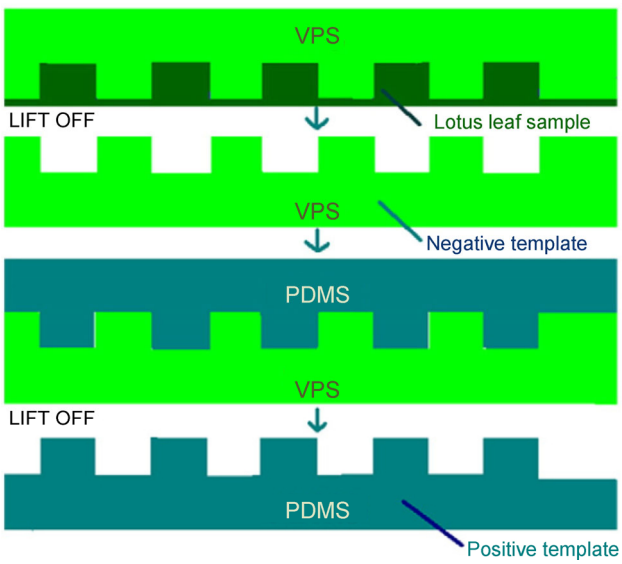

Fig. 3 Schematic illustration of direct replication and process sequence [31].

3.2 Chemical wet etching

Wet etching, also known as chemical wet etching or liquid etching, uses liquid chemicals or etchants to perform a material removal process on the sample [32–34]. The predefined masks with desired textures are attached to the sample surface before the chemical wet etching process. Usually, these masks are pre-fabricated by using lithography technique [35]. During the etching process, the surface regions not covered by the masks are etched away to produce deterministic textures. Meanwhile, multiple chemical reactions are performed which involve three steps: diffusion of the etchant to the material surface which is not covered by the mask; the chemical reactions between the etchant and the materials have been etched away; Secondary diffusion of the reacted sample surface.

Chemical wet etching methods can be categorized into two types: anistropic and isotropic [36, 37]. Both processes have different etching rates which depend on the material properties of the sample. The most common application of anistropic wet etching method is applied for the fabrication of crystalline materials [38, 39]. The etching rate varies base on the plane of the crystalline material and the concentrations of the etchants. For instance, crystalline material like silicon may have high anisotropic effect by using etchants, e.g., potassium hydroxide (KOH), ethylenediamine pyrocatechol (EDP), tetramethylammonium hydroxide (TMAH), etc. The typical applications for anisotropic wet etching are J-FET arrays, solar cell anti-reflecting surfaces and waveguides.

In 1983, a series of electrochemical measurements of n- and p-type Si wafers with crystal plane of {1 0 0} and {1 1 1} were analyzed to study the importance of the orientation dependent etching [40]. Potassium hydroxide (KOH) was used as etchant for the anisotropic wet etching process. Researcher [41] attempted to study the reaction mechanism and key features of all alkaline anisotropic etchants upon silicon materials. In the study, experimental data were analyzed base on the anisotropy, selectivity and voltage dependence of anisotropic etchants. In the conclusion, the concentration of molar water and pH value are the two key parameters for the etching behaviour of alkaline solutions. In 1995, a research group in IBM's Microelectronics Division, USA [42], was using an etchant

consisting of ethanolamine, gallic acid, surfactant, catalyst and water for anistropic wet etching on the three major crystal planes of silicon. The objective was to study the catalytic control of anisotropic wet etching rate. During the experiments, chemical etching method was strongly influenced by a variety of oxidative catalysts. The results were categorized into three groups by how fast catalysts can accelerate the chemical etching rate of a specific crystal plane compared to the uncatalyzed rate: two to five times; less than twice and below the uncatalyzed level.

Different from anisotropic wet etching process, the etching rate is same in all direction for isotropic wet etching [43]. It is suitable for removal of pre-damaged surfaces, rounding of pre-etched sharp corners, fabricating the structures on single-crystal lattices, and producing large geometries. Similar to anisotropic wet etching process, the plane of the crystalline material and the concentrations of etchant are the important factors for etching rate in isotropic wet etching process. The common etchant is the mixture of hydrofluoric acid (HF), nitric acid and acetic acid for crystalline materials. The etching rate is affected by the concentration of each chemical etchant. In some researches, isotropic wet etching was combined with laser surface texturing technique [44]. The concave micro lens arrays were fabricated by a third harmonic Nd: YAG laser on a gold film which coated on a glass substrate. Followed by the isotropic wet etching process, the exposed area on glass substrate was etched by using hydrofluoric acid solutions (refer to Fig. 4). In the study, the effects of various types of HF solutions on etching efficiency were analyzed.

Recently, a research group applied isotropic wet etching technique to fabricate desired texture for light guidance application [36]. HNA based etchant solution is used to produce the surface structure of 300 μm deep channel with smooth wall. The etchant composition was selected by surface quality of etching process and etching rate. A spin etcher tool was used to further reduce the surface roughness. This method was able to produce deep isotropic channels in optical quality (refer to Fig. 5).

3.3 Plasma etching

Plasma etching is a mature technique specific for the fabrication of microsystems and surface texturing [45]. From the mid-1960s, the mechanisms of plasma etching were first introduced as a revolutionary technique for the fabrication of integrated circuit [46]. In the 1970s, it was widely accepted and expected to be an important fabrication technique in the industry of semiconductor and other applications requiring fine-line lithography [47]. In general, plasma etching undergoes a chemical reaction between the solid atoms from the substrate material and gas atoms from the gas etchant. The gas etchants are in the form of molecules, but not chemically reactive enough to fabricate the material surface. The role of plasma is to dissociate the molecules of the gas etchant into reactive atoms in order to be sufficient in the task of

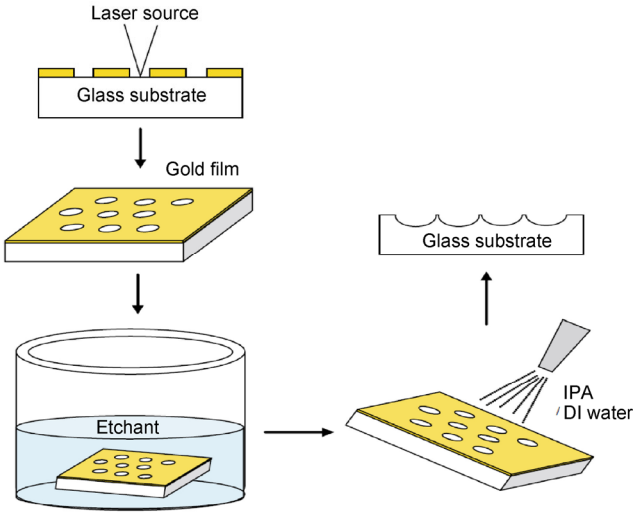

Fig. 4 Schematic of the etching process flow [44].

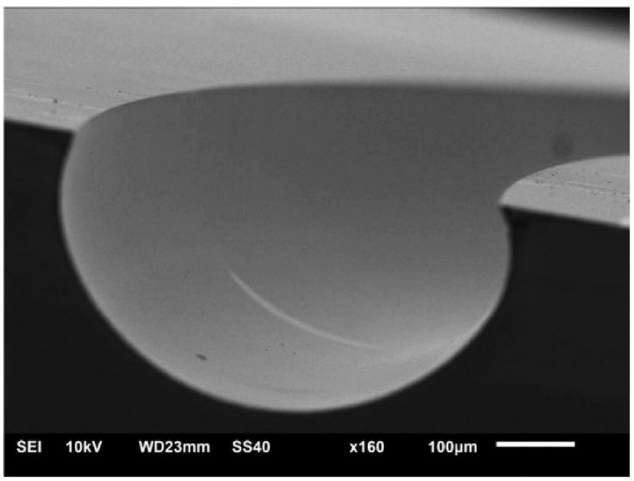

Fig. 5 Image of a 300 μm deep channel which has a channel wall in optical quality [36].

fabrication. Over the years, various plasma etching techniques are introduced, and radio frequency (RF) sputter etching technique is still the most common and core plasma etching technique for surface texturing.

The radio frequency (RF) sputter etching method was first introduced from IBM [48], and was found to be very useful for fabricating thin film resistors on Cr-SiO films. The $1^1/_4$ inch silicon wafers were used as the substrates pre-coated film with a 1.5 μ thickness. Kodak thin film resist (KTFR) was used as the resist through the sputter etching (refer to Fig. 6). From the results, RF sputter etching demonstrated its universality and ability to prevent under-cutting. This technique is able to etch any kinds of substrates with standard photoresist. Later, fluorine and chlorine-containing gas etchants were introduced to RF sputter etching [49]. The compositions of gas etchants are CF_4, CCl_2F_2, CCl_3F, $CHCl_2F$, $CHClF_2$, $(CCl_2F)_2$, CCl_2FCClF_2 and $(CBrF_2)_2$. The etching rate is enhanced by using fluorine and chlorine-containing gas etchants on Si, quartz, glass, Al, Mo, stainless steel and photoresist. From the results, RF sputter etching method with fluorine and chlorine-containing gas etchants is characterized as a high rate, precise and dry etching technique.

Recently, the work from Aizawa and Fukuda developed a high-density RF-DC plasma etching system (OXP-1; YS-Electrics, CO. Ltd.) to fabricate the diamond-like carbon (DLC) coating via PVD/CVD on the SKD11 substrate (refer to Fig. 7) [50]. The oxygen gas instead of hazardous etchants such as CF_4 was attained with high etching rate. During the etching process, the specimens were fixed on the cathode table before evacuation down to the base pressure of 0.1 Pa. The chamber was filled with a carrier gas to attain the specific pressure. With the use of magnetic

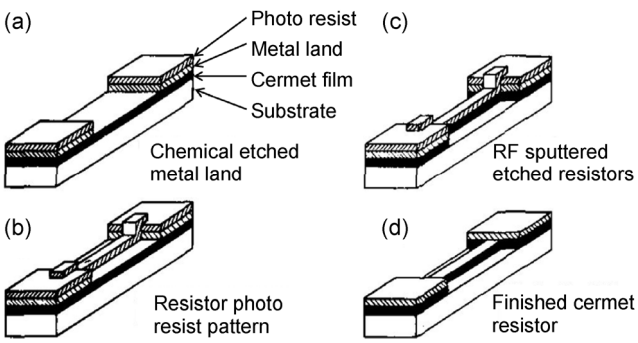

Fig. 6 Sputter-etching of thin-film resistors [48].

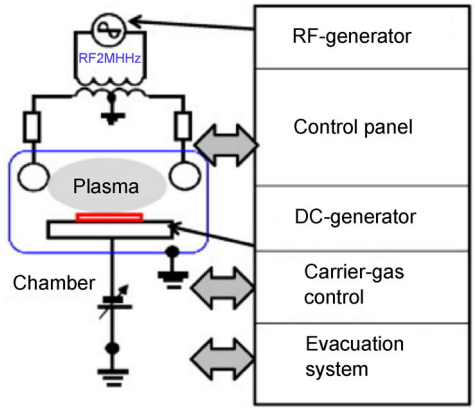

Fig. 7 Schematic diagram of high-density plasma etching system [50].

lens, the ignited RF-DC oxygen plasmas were focused onto the surface of specimens during etching. The RF-voltage, DC bias and pressure were selected to be 250−450 V and 25 to 40 Pa respectively.

3.4 Three-dimensional printing

Three-dimensional printing (3DP) is a revolutionary bottom-up fabrication technique. Compared to traditional top-down fabrication techniques, it has many advantages like moldless production, cheap manufacturing, less waste and the ability to produce complex structures. The method was introduced by Charles Hull and first known as stereolithography in 1980s [51]. Early 3D printing method spreaded the material powder layer by layer and used binder material printed by ink-jet to selectively bind the powder in order to produce the parts [52]. After all the layers were finished, the unused powder was removed to complete the process (refer to Fig. 8). The parts were designed by CAD with complete freedom in complex geometry, surface texture and material composition. The potential material selection includes any materials which are available in a particle sized powder form, e.g., polymers, metals and ceramics [53−56].

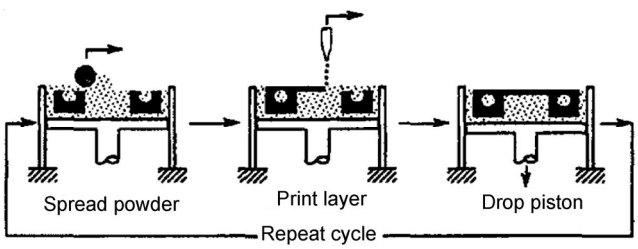

Fig. 8 The sequence of the operations in 3D Printing [52].

Recently, a new developed super-resolution 3D printing system was introduced by using electrohydrodynamic (EHD) method [57]. It was able to directly fabricate micro-structures on the substrate surface with phase-change inks. The material of phase-change ink was wax which can be quickly solidified under room temperature after printed onto the substrate surface. The printing system consists of a XYZ precision stage, a thermal control unit, a pneumatic dispensing system and a high voltage supply (refer to Fig. 9). The formation and size of droplet can be predicted by finite element analysis (FEA) model. The EHD 3D printing technique is capable of fabricating high aspect-of-ratio and high resolution (sub-10 μm) surface structures (refer to Fig. 10).

3.5 Laser surface texturing

Laser surface texturing (LST) in particular is regarded as an important technique to enhance tribological performance [58]. Over the decades, many researchers [59–61] studied LST. In 1997, a research group was applying neodymium-yttrium aluminum garnet (Nd-YAG) pulsed solid-state laser to modify the surface of aluminum alloys [62]. The Nd-YAG laser emitted at a wavelength of 1.06 μm and two main surface features were produced: the non-periodic concentric ring structure and the micro-crack pattern. From the experimental results, both ring structure and micro-crack could be tailored (pre-defined) to a certain extent in order to improve the adhesive bonding of aluminum alloys. One year later, a research group led by Geiger [63] fabricated microstructures on ceramic surfaces by excimer laser radiation to improve the tribological properties under hydrodynamic and elastohydrodynamic sliding conditions (refer to Fig. 11). Ceramics obtain extremely high hardness, temperature

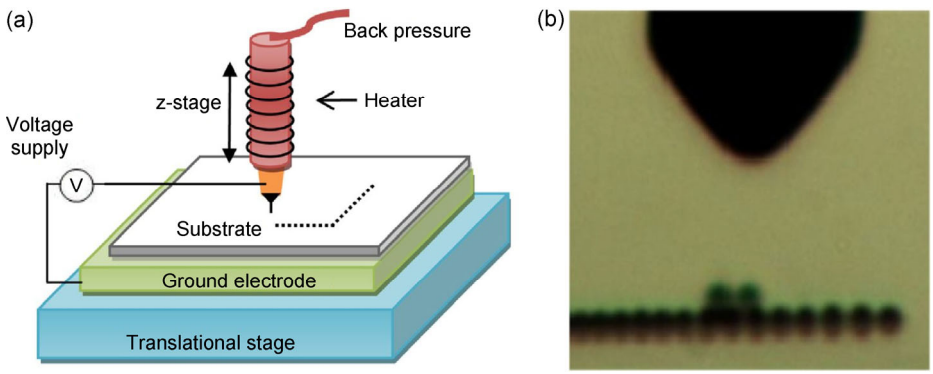

Fig. 9 (a) Schematic of the EHD 3D printing set-up system; (b) pulsating mode of EHD 3D printing of wax [57].

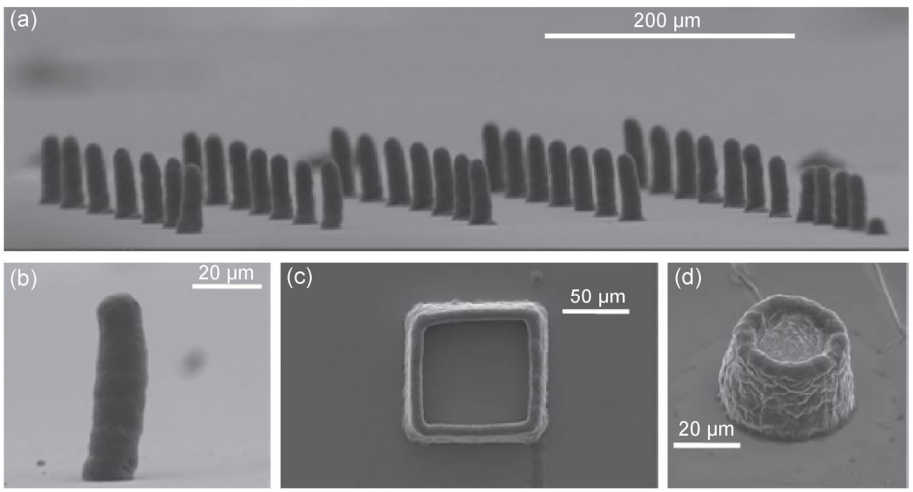

Fig. 10 Micro-structures printed from EHD 3D printing process. (a) Micro-pillar array; (b) close view of a single pillar; (c) square with thin wall; (d) circular tube with thin wall [57].

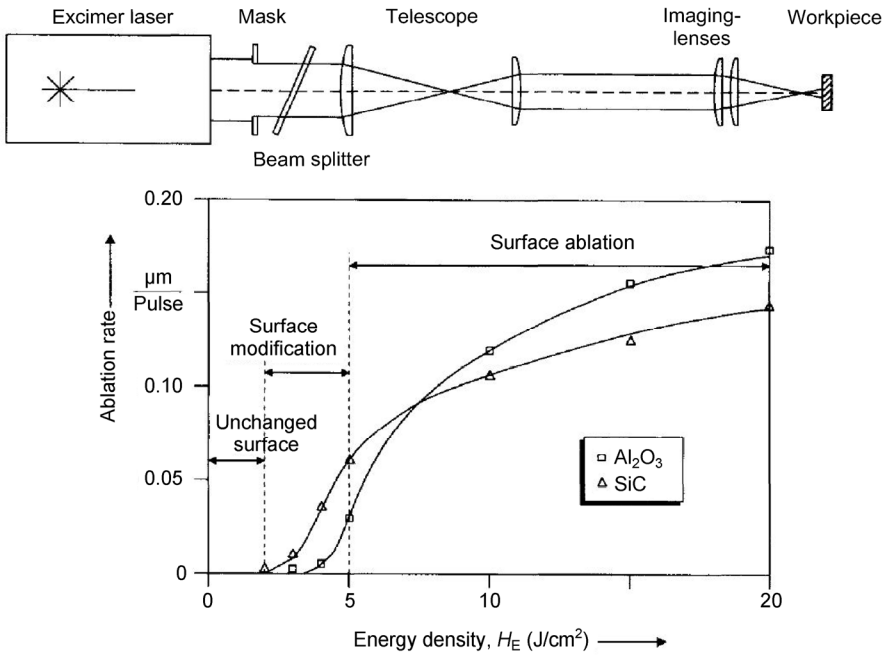

Fig. 11 Micro-structuring of ceramics by XeCl eximer laser radiation [63].

resistance and corrosion resistance. These material properties made ceramics an excellent choice for the application of wear and sliding. Excimer laser processing offers innovative ways to produce textures on ceramics. Pulsed radiation emitted by excimer lasers are in the UV range of the electromagnetic spectrum. In particular, excimer lasers are effective for fabricating microstructures with high resolution. This is benefitted by the short wavelength (λ = 193–351 nm) and small penetration depth of excimer laser radiation. This method is able to modify the surface topography of ceramics by changing surface roughness (Ra), even fabricate microstructures with pre-defined geometric properties to have positive influences on the sliding properties, and increase lubricant film thickness or serve as lubricant reservoirs.

In 2002, the same group [64] was using a mask illuminated by laser beam to project its geometrical information onto the surface (refer to Fig. 12) and

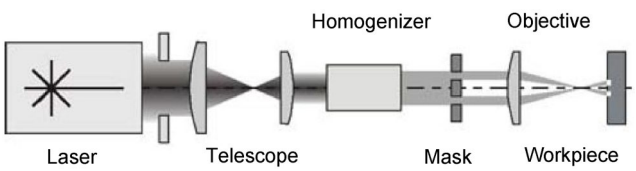

Fig. 12 Principle of the beam guiding system of an excimer laser for use with masks [64].

focusing on the influence of micro textures by excimer laser method on the tribological behaviour of tools in cold forging process. A punch was applied in this method to produce rivets and improve cold forging tool life up to 169%.

A CO_2 laser was used to fabricate micro-pores on SiC surfaces by a research group in Tohoku University [65]. Various textured specimens fabricated with different intervals between the micro-pores were tested and compared to non-textured specimen (refer to Fig. 13). The effect of the micro-pore area ratio on friction coefficient and the critical load for transition from hydrodynamic to mixed lubrication regime were studied. More extensive research works on LST were done at Argonne National Laboratory, USA [66, 67] to further understand the effect of micro-structures fabricated by LST on the transition from boundary to hydrodynamic lubrication regime. Friction and electrical-contact resistance were measured by a pin-on-disk setup in unidirectional sliding conformal contact (refer to Fig. 14). The experimental results illustrated that the range of the hydrodynamic lubrication regime is expanded by LST in terms of load and sliding speed. In addition, micro-dimples produced by LST were able to perform a significant reduction of the friction coefficient compared to non-textured surfaces.

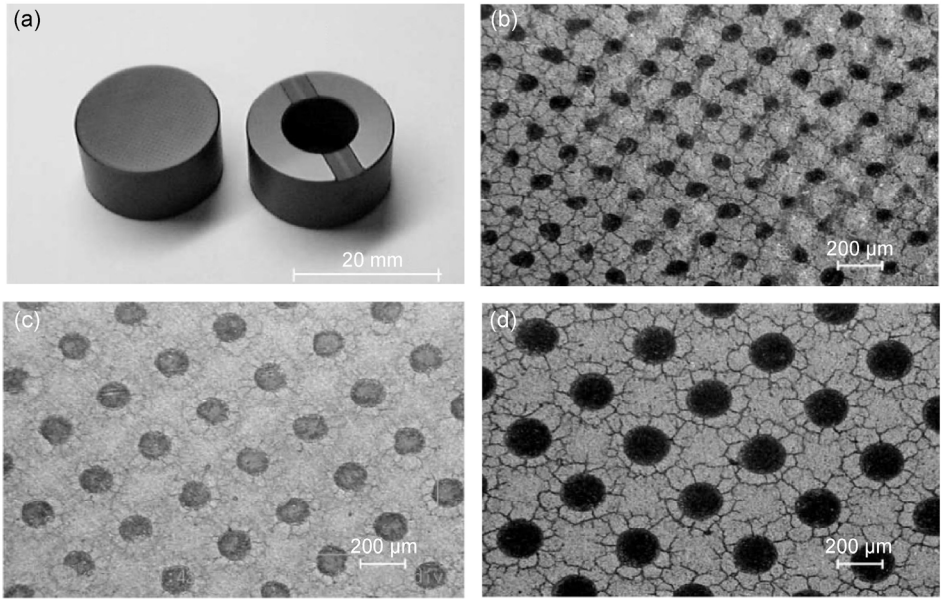

Fig. 13 (a) Appearance of disk (left) and cylinder (right). Optical micrographs of pores on the disk surface produced by laser texturing: (b) the pores with diameter of 100 μm; (c) the pores with diameter of 150 μm; (d) the pores with diameter of 200 μm [65].

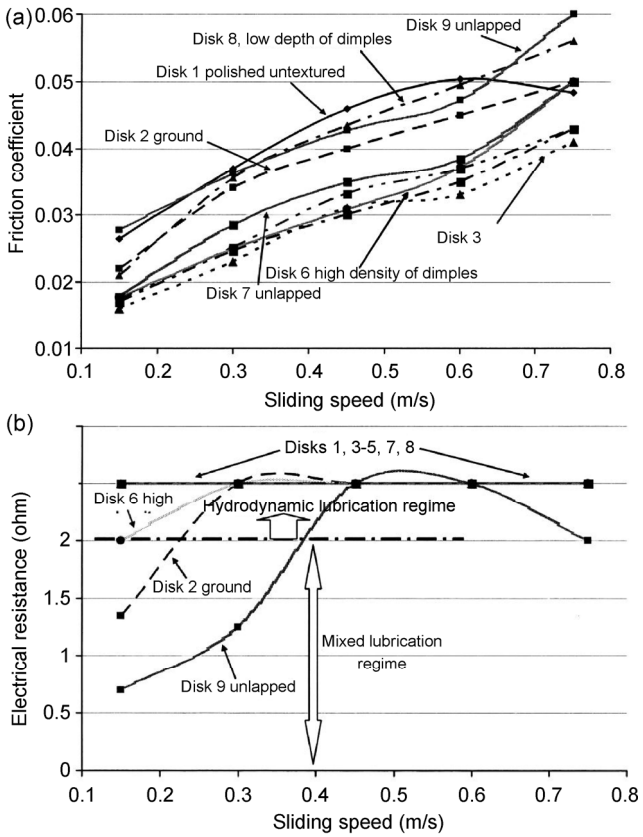

Fig. 14 (a) Friction coefficients; (b) electrical resistance between flat-pin and tested disks as a function of sliding speed at 5 N load and higher viscosity oil lubricant [66].

Furthermore, the application of LST has been expanded to bio-tribology in the recent years. In the Netherlands, samples with well-defined surface topography were used to unlock the "feel" of surfaces by an experimental study on the relation between surface texture and tactile friction [68]. The micro-geometries of the metal samples were fabricated by picosecond laser pulses, also used as injection molds for thermoplastic polyurethane (TPU) samples in experimental work (refer to Fig. 15). Friction measurements of skin against textured samples were carried out by using a load cell (ATI Gamma three-axis force/torque transducer, ATI Industrial Automation, Apex, NC, USA). Under different normal loads, the coefficient of friction strongly decreased for both textured metal and TPU samples. In the further research, the role of the skin microrelief in the contact between finger and laser textured surfaces was studied [15]. An experimental approach on the friction behavior of the finger pad as a function of asperity geometry was investigated. The surface textures used *in vivo* testing were fabricated by LST to have evenly distributed asperities with spherical tips. A new multi-scale model was developed to analytically explain skin friction behavior as a function of texture geometry, normal

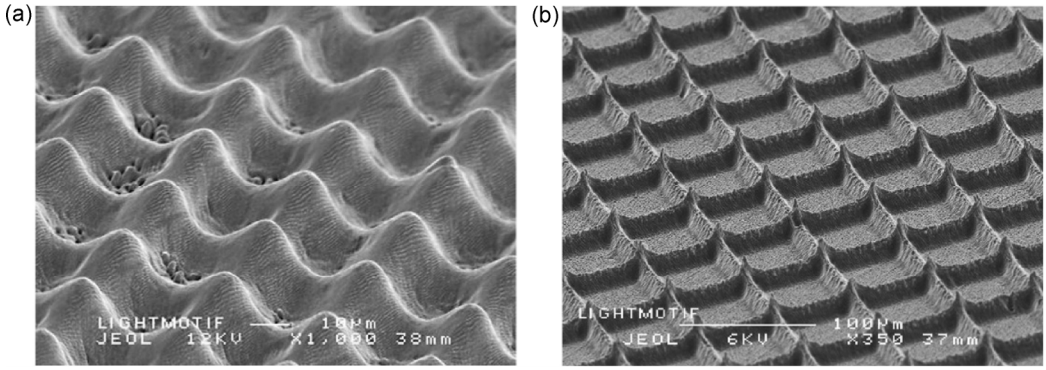

Fig. 15 SEM image (a) metal sample with tip radius R = 5 μm and spacing λ = 30 μm; (b) TPU sample with tip radius R = 1 μm and spacing λ = 60 μm [68].

load and skin properties. From the observations of *in vivo* measurements, the coefficient of friction (COF) was found to increase with the increment of asperity tip radius. With increasing asperity density, COF increased as well. By using relatively simple analytical expressions, the skin friction behavior may be estimated as a function of asperity geometry and operational conditions. Also, LST was proven to be a useful technique to fabricate well-defined micro-textures to study skin-tribology related researches.

4 Discussion

It is important to discuss the feasibility of fabrication techniques for stainless steel. From the review of state-of-art fabrication techniques, the pulsed laser surface texturing (LST) is considered as the most suitable method for producing the desired surface structure on the stainless steel sheets (refer to Table 1), i.e., directly by laser ablation. Picosecond and nano-second lasers can be employed to create specific

Table 1 The advantages and disadvantages of chemical wet etching, plasma etching, LST and 3D printing.

Methods	Advantages	Disadvantages
Micro-casting	• Cheap • Low cost • Complex 3D component	• Need other micro-fabrication techniques to produce the mold
Chemical wet etching	• Low cost, simple process • Highly selectivity • Controllable etching rate	• Chemical Contamination • Orientation dependent (the plane of the crystalline) • Poor repeatability based on the influences of temperature and concentration of etchant • Undercutting.
Plasma etching	• High feature resolution • Easy to control • High reproducibility • No liquid chemical waste	• High cost • Poor selectivity • Potential radiation damage
LST	• Dry process with physical contact • Automated process • Precise control of etching depth • Able to fabricate on metallic workpiece	• time consuming • high cost
3D printing	• Complex structures • Low cost • Rapid prototyping • Automated process	• Limited raw materials • Low feature resolution

topographic features [69], such as grids (picosecond laser), crater (nanosecond laser), and groove (nanosecond laser) patterns with different surface parameters. Secondly, specific operational conditions can be used for texture design aspects.

However, LST is a rather time consuming and high cost fabrication technique. For this reason, stamping (or pressing) and cold rolling, which are low cost with fast production rate, can be applied for the micro-fabrication with textured stamping dies and textured cold rolling rolls by LST. Full upscaling of the process is required to gauge the applicability of the laser texturing process to industrial stamping die. Primarily, a TUWI compression rig was used for stamping process at Tata Steel (refer to Fig. 16) [69]. In the first stage, the roughness transfer capability needs to be evaluated. After an initial texture pattern was considered, the imprinting tests were carried out. For texturing the cold rolling rolls, a 6-axis robot was used by IK4-TEKNIKER along with a rotary axis during the laser texturing process. Primarily, Tata Steel Pilot Mill (named the MultiMill) (refer to Fig. 17) in 4-high mode was used for the cold rolling. The textured work rolls are driven and supported by back-up rolls. The strip was hand-fed in 150 mm wide strips with length of 500 mm to 1,000 mm. As a result, the stainless steel sheet was fabricated with the designed textures by LST, stamping and cold rolling techniques. The surface texture of samples was examined by SEM and confocal microscope (refer to Fig. 18).

The dynamic sliding friction between the skin and samples was measured by a multi-axis force/torque

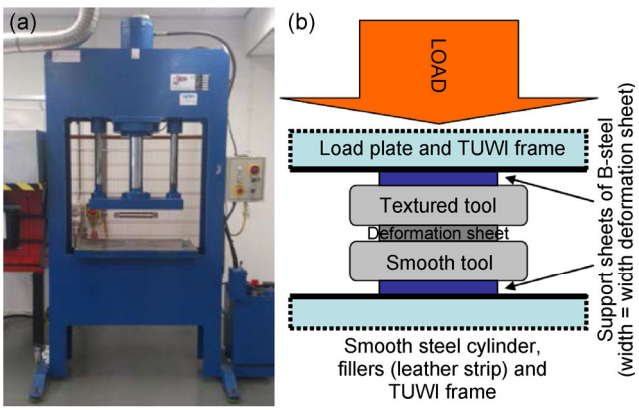

Fig. 16 (a) Overview of the TUWI compression rig used for stamping, and (b) schematic of the key aspects of the set-up at Tata Steel within the STEELTAC project [69].

Fig. 17 Overview of the pilot rolling mills at Tata Steel, used for rolling trials in Steeltac: (left) 4-high Multimill, and (right) 2-high "Bühler" mill, used for the STEELTAC project [69].

transducer (ATI Industrial Automation, Apex, NC, USA). One conventionally finished sample (2G finish) was conducted in the same friction measurement as a reference sample for comparison. The testing finger belongs to an adult male (32 year-old) with no-known skin disease. The same finger (middle finger of left hand) was used for all texting samples during the measurements. The stroke length was 30 mm and the sliding velocity was kept as constant as possible with an average of 44.3 mm/s.

Base on the results of friction measurements, the average COFs of micro-structured samples with pre-defined deterministic textures ranged from 1.05 to 1.26 compared to the reference sample with COF of 3.64 ± 1.04 (refer to Table 2). As shown in Figs. 19(a)&(b), the micro-structured samples including laser surface textured, stamped and cold rolled samples significantly decreased the friction force between the skin and counter-surfaces compared to the reference sample. The results validated that the pre-defined deterministic surface textures on stainless steel sheet produced by laser surface texturing, stamping and cold rolling fabrication techniques can greatly influence the friction between the skin and counter-surface, in this case, the skin friction was greatly reduced.

5 Conclusion

Micro-casting, chemical wet etching, plasma etching, laser surface texturing and 3D printing are the major fabrication methods to produce predefined deterministic surface structures in micro scale detail. In addition, micro-casting and 3D printing are able to produce complicated 3D components. In comparison,

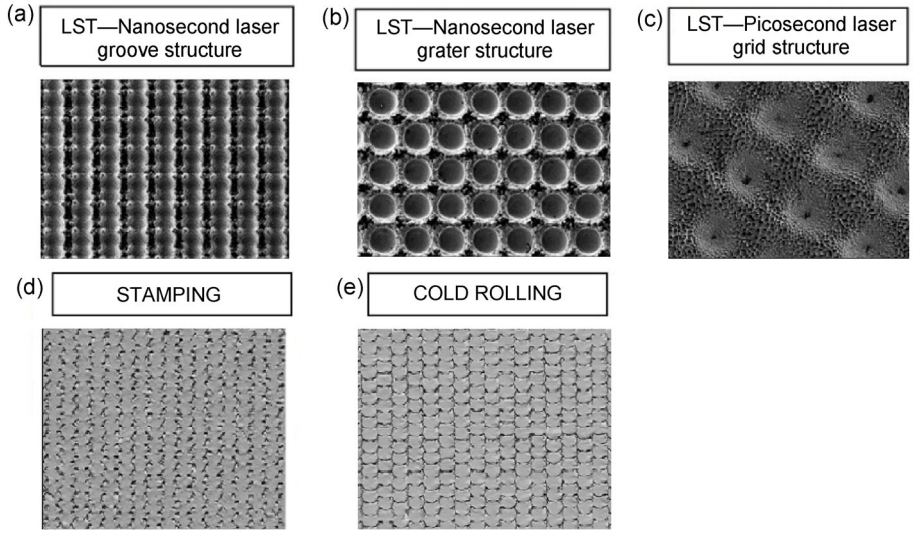

Fig. 18 SEM images of samples (a) crater, (b) groove and (c) grid patterns; confocal microscope image of sample: (d) stamped and (e) cold rolled samples [69].

Table 2 Friction measurements of all samples.

Sample name	Normal force (N)	Friction force (N)	COF
Groove (NS)	0.12 ± 0.03	0.13 ± 0.03	1.09 ± 0.09
Crater (NS)	0.18 ± 0.05	0.19 ± 0.06	1.05 ± 0.82
Grid (PS)	0.13 ± 0.04	0.15 ± 0.05	1.26 ± 0.55
Crater (Stamped)	0.16 ± 0.03	0.19 ± 0.07	1.23 ± 0.37
Crater (Cold Rolled)	0.18 ± 0.04	0.21 ± 0.06	1.18 ± 0.28
2G (Reference)	0.15 ± 0.04	0.51 ± 0.16	3.64 ± 1.04

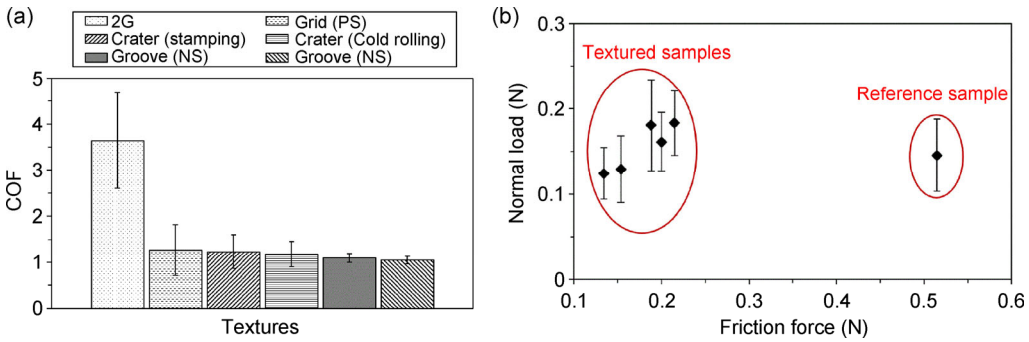

Fig. 19 (a) The average values of COF of the dynamic friction measurements; (b) the average normal load versus friction force.

3D printing is a relatively new method, and its innovative method of bottom-up processing offers the potential to completely revolutionize the process of surface texturing. In this review, the mechanism and application of all five categories of surface texturing techniques are introduced, and each method has its advantages and disadvantages (refer to Table 1). Also, it is important to understand that one method may be more appropriate than the other in a given application or producing a specific surface structure.

The needs for the surface structures in industrial and scientific fields are not stalled, and the surface texturing techniques are always evolving. From chemical wet etching to 3D printing, or from a

traditional method to a revolutionary bottom-up rapid processing method, surface texturing techniques are improving and innovating continuously.

In this paper, LST is chosen to be the main fabrication method for producing the surface texture due to its accuracy and ability to fabricate on stainless steel sheet material. For large production, the industrial stamping and cold rolling processes can be used, based on imprinting the negative of the design, to lower the cost and fabrication time. Again, LST has proven its feasibility in creating the negative at the involved forming tools, although only at laboratory scale yet. Based on the friction measurement tests, the predefined deterministic textures greatly reduced the dynamic friction between the skin and micro-structured samples compared to the reference sample which has a stochastic surface.

Acknowledgements

This work was supported by the Research Programme of the Research Fund for Coal and Steel (Contract No. RFSR-CT-2011-00022).

References

[1] Wiklund D. Tribology of stamping the influence of designed steel sheet surface topography on friction. PhD Thesis. Chalmers Tekniska Hogskola, Gothenburg, Sweden, 2006.

[2] Pettersson U, Jacobson S. Influence of Surface Texture on Boundary Lubricated Sliding Contacts. *Tribol Int* **36**: 857–864 (2003)

[3] Sugihara T, Enomoto T, Crater and Flank. Wear resistance of cutting tools having micro textured surfaces. *Precision Engineering* **37**(4): 888–896 (2013)

[4] Tang W, Zhou Y K, Zhu H, Yang H F. The effect of surface texturing on reducing the friction and wear of steel under lubricated sliding contact. *Appl Surf Sci* **273:** 199–204 (2013)

[5] Ling F F. Fractals, engineering surfaces and tribology. *Wear* **136**: 141–156 (1990)

[6] Zahouani H, Vargiolu R, Loubet J L. Fractal models of surface topography and contact mechanics. *Mathematical and Computer Modelling* **28**: 517–534 (1998)

[7] Bruzzone A A G, Costa H L. Functional characterization of structured surfaces for tribological applications. *Procedia CIRP* **12**: 456–461 (2013)

[8] Ibatan T, Uddin M S, Chowdhury M A K. Recent development of surface texturing in enhancing tribological performance of bearing sliders. *Surf Coat Technol* **272**: 102–120 (2015)

[9] Wiklund D, Rosen B G, Gunnarsson L. Frictional mechanisms in mixed lubricated regime in steel sheet metal forming. *Wear* **264**: 474–479 (2008)

[10] Groenendijk M N W, Meijer J. Surface microstructures obtained by femtosecond laser pulses. CIRP *Annals* **55**(1): 183–186 (2006)

[11] Yan X, Li W, Aberle G A, Venkataraj S. Investigation of the thickness effect on material and surface texturing properties of sputtered ZnO:Al films for thin-film Si solar cell applications. *Vacuum* **123**:151–159 (2016)

[12] Khatri B C, Sharma C S. Influence of textured surface on the performance of non-recessed hybrid journal bearing operating with non-newtonian lubricant. *Tribol Int* **95**: 221–235 (2016)

[13] Yu S S, Zhang S, Xia Z W, Liu S, Lu H J, Zeng X T. Textured hybrid nanocomposite coatings for surface wear protection of sports equipment. *Surf Coat Technol* **287**: 76–81 (2016)

[14] Barnes C J, Childs T H C, Henson B, Southee C H. Surface finish and touch—A case study in a new human factors tribology. *Wear* **257**: 740–750 (2004)

[15] Van Kuilenburg J, Masen M A, van der Heide E. The role of the skin microrelief in the contact behaviour of human skin: Contact between the human finger and regular surface textures. *Tribol Int* **65**: 81–90 (2013)

[16] Klatzky R L, Pawluk D. Haptic perception of material properties and implications for applications. *Proceedings of the IEEE* **101**: 2081–2092 (2013)

[17] Klatzky R L, Lederman S J. Tactile roughness perception with a rigid link interposed between skin and surface. *Perception & Psychophysics* **61**: 591–607 (1999)

[18] Skedung L, Danerlov K, Olofsson U, Johannesson C M, Aikala M, Kettle J, Arvidsson M, Berglund B, Rutland M W. Tactile perception: Finger friction, surface roughness and perceived coarseness. *Tribol Int* **44**: 505–512 (2011)

[19] Skedung L, Arvidsson M, Chung J Y, Stafford C M, Berglund B, Rutland M W. Feeling small: Exploring the tactile perception limits. *Sci Rep* **3**: 1–6 (2013)

[20] Tomlinson S E, Carre M J, Lewis R, Franklin S E. Human finger contact with small, triangular ridged surfaces. *Wear* **271**: 2346–2353 (2011)

[21] Veijgen N K. Skin friction: A novel approach to measuring in vivo human skin. PhD Thesis. University of Twente, Enschede, the Netherlands, 2013.

[22] Derler S, Huber R, Feuz H P, Hadad M. Influence of surface microstructure on the sliding friction of plantar skin against hard substrates. *Wear* **267**(5–8): 1281–1288 (2009)

[23] Adams M J, Briscoe B J, Johnson S A. Friction and lubrication of human skin. *Tribol Lett* **26**(3): 239–253 (2007)

[24] Duvefelt K, Olofsson U, Johannesson C M, Skedung L. Model for contact between finger and sinusoidal plane evaluate adhesion and deformation component of friction. *Tribol Int* **96**: 389–394 (2016)

[25] Prodanov N, Gachot C, Rosenkanz A, Muchlich F, Muser M H. Contact mechanics of laser-textured surfaces. *Tribol Lett* **50**: 41–48 (2013)

[26] Khodai M, Parvin N. Pressure measurement and some observation in lost foam casting. *J Mater Process Technol* **206**(1–3): 1–6 (2008)

[27] Li J, Chen R, Ke W. Microstructure and mechanical properties of Mg-Gd-Y-Zr alloy cast by metal mould and lost foam casting. *Transactions of Nonferrous Metals Society of China* **21**(4): 761–766 (2011)

[28] Ferro P, Fabrizi A, Cervo R, Carollo C. Effect of inoculant containing rare earth metals and bismuth on microstructure and mechanical properties of heavy-section near-eutectic ductile iron castings. *J Mater Process Technol* **213**(9): 1601–1608 (2013)

[29] McGinley E L, Moran G P, Fleming G J P. Biocompatibility effects of indirect exposure of base-metal dental casting alloys to a human-derived three-dimensional oral mucosal model. *Journal of Dentistry* **41**(11): 1091–1100 (2013)

[30] Li B, Ren M, Yang C, Fu H. Microstructure of Zn-Al4 alloy microcastings bymicro precision casting based on metal mold. *Transactions of Nonferrous Metals Society of China* **18**: 327–332 (2008)

[31] Adithyavairavan M, Subbiah S. A morphological study on direct polymer cast micro-textured hydrophobic surfaces. *Surf Coat Technol* **205**: 4764–4770 (2011)

[32] Chao B, Cheng H, Nien L, Chen M, Nagao T, Li J, Hsueh C. Anti-reflection textured structures by wet etching and island lithography for surface-enhanced raman spectroscopy. *Appl Surf Sci* **357**(A): 615–621 (2015)

[33] Chen W, Lin J, Hu G, Han X, Liu M, Yang Y, Wu Z, Liu Y, Zhang B. GaN nanowire fabricated by selective wet-etching of gan micro truncated-pyramid. *Journal of Crystal Growth* **426**: 168–172 (2015)

[34] Kumar M D, Kim H, Kim J. Periodically patterned si pyramids for realizing high efficient solar cells by wet etching process. *Solar Energy* **117**: 180–186 (2015)

[35] Jaeger R C. *Introduction to Microelectronic Fabrication, 2 ed.* Auburn, Upper Saddle River-Prentice Hall, 2002.

[36] Bauhuber M, Mikrievskij A, Lechner A. Isotropic wet chemical etching of deep channels with optical surface quality in silicon with hna based etching solution. *Mater Sci Semiconduct Process* **16**: 1428–1433 (2013)

[37] Mondiali V, Lodari M, Chrastina D, Barget M, Bonera E, Bollani M. Micro and nanofabrication of SiGe/Ge bridges and membrances by wet-anisotropic etching. *Mciroelectr Eng* **141**: 256–260 (2015)

[38] Reshak A H, Shahimin M M, Shaar S, John N. Surface modification via wet chemical etching of single-crystalline silicon for photovoltaic application. *Progress in Biophysics and Molecular Biology* **113**(2): 327–332 (2013)

[39] Lee Y, Kim H, Hussain S Q, Han S, Balaji N, Lee Y, Lee J, Yi J. Study of metal assisted anisotropic chemical etching of silicon for high aspect ratio in crystalline silicon solar cells. *Mater Sci Semiconduct Process* **40**: 391–396 (2015)

[40] Faust J W, Palik E D. Study of the orientation dependent etching and initial anodizationg of Si in aqueous KOH. *J Electrochem Soc* **130**: 1413–1420 (1983)

[41] Seidel H. The mechanism of anisotropic, electrochemical silicon etching in alkaline solutions. IEEE In *Solid-State Sencor and Actuator Conference*, 1990: 86–91.

[42] Linde H G, Austin L W. Catalytic control of anistropic silicon etching. *Sensors and Actuators A* **49**: 181–185 (1995)

[43] Sheeja D, Tay B K, Yu Y J, Chua D H C, Milne W I, Miao J, Fu Y Q. Fabrication of amorphous carbon cantilever structures by isotropic and anisotropic wet etching methods. *Diamond and Related Materials* **12**(9): 1495–1499 (2003)

[44] Lim C S, Hong M H, Senthil Kumar A, Rahman M, Liu X D. Fabrication of concave micro lens array using laser patterning and isotropic etching. *International Journal of Machine Tools & Manufacture* **46**: 552–558 (2005)

[45] Freires de Queiroz J D, Maria de Sousa Leal A, Terada M, Agnez-Lima L F, Costa I, Cristhina de Souza Pinto N, Batistuzzo de Medeiros S R. Surface Modification by argon plasma treatment improves antioxidant defense ability of CHO-k1 cells on titanium surfaces. *Toxicology in Vitro* **28**: 381–387 (2014)

[46] Donnelly V M, Kornblit A. Plasma etching: Yesterday, today, and tomorrow. *Journal of Vacuum Science & Technology A* **31**(5): 1–48 (2013)

[47] Coburn J W, Winters H F. Plasma etching—A discussion of mechanisms. *Journal of Vacuum Science & Technology* **16**: 391 (1979)

[48] Davidse P D. RF sputter etching—A universal etch. *Journal of Electrochemical Society: Solid State Science* **116**(1): 100–103 (1969)

[49] Hosokawa N, Matsuzaki R, Asamaki T. RF sputter-etching by fluoro-chloro-hydrocarbon gases. *Japanese Journal of Applied Physics* **13**: 435–438 (1974)

[50] Aizawa T, Fukuda T. Oxygen Plasma etching of diamond-like carbon coated mold-die for micro-texturing. *Surf Coat Technol* **215**: 364–368 (2013)

[51] 3D Systems Inc. Company set up for stereolithography. *CAD in Industry* 19(4): 223 (1987)

[52] Sachs E, Cima M, Cornie J, Brancazio D, Bredt J, Curodeau A, Fan T, Khanuja S, Lauder A, Lee J, Michaels S. Three-dimensional printing; the physics and implications of additive manufacturing. *CIRP Annals—Manufacturing Technology* **42**(1): 257–260 (1993)

[53] Lam C X F, Mo X M. Scaffold development using 3D printing with a starch-based polymer. *Materials Science & Engineering, C: Biomimetic and Supramolecular Systems C* **20**(1–2): 49–56 (2002)

[54] Moon J, Caballero J E. Ink-jet printing of binders for ceramic components. *Journal of the American Ceramic Society* **85**(4): 755–762 (2002)

[55] Seitz H, Rieder W. Three-dimensional printing of porous ceramic scaffolds for bone tissue engineering. *Journal of Biomedical Materials Research, Part B, Applied Biomaterials* **74**(2): 782–788 (2005)

[56] Utela B, Storti D, Anderson R, Ganter M. A review of process development steps for new material systems in three dimensional printing (3DP). *J Manufact Process* **10**: 96–104 (2008)

[57] Han Y, Wei C, Dong J. Super-resolution electrohydrodynamic (EHD) 3D printing of micro-structures using phase-change inks. *Manufact Lett* **2**: 96–99 (2014)

[58] Dunn A, Wlodarczyk K L, Carstensen J V, Hansen E B, Gabzdyl J, Harrison P M, Shephard J D, Hand D P. Laser surface texturing for high friction contacts. *Applied Surface Science* **357**(B): 2313–2319

[59] Kurella A, Dahotre B N. Review paper: Surface modification for bioimplatns: The role of laser surface engineering. *Journal of Biomaterials Applications* **20**: 5–50 (2005)

[60] Wang Y, Yang H, Hao J, Han Q, Fang L, Ge S. Experiment research on fabrication & wettability of micro- and nano-scale surface textured by ultrafast laser. *Lasers In Engineering* **21**(3-4): 241–254 (2011)

[61] Kumari R, Scharnweber T, Pfleging W, Besser H, Majumdar J D. Laser Surface textured titanium alloy (Ti-6Al-4V)—Part II—Studies on bio-compatibility. *Appl Surf Sci* **357**(A): 750–758 (2015)

[62] Wong RCP, Hoult AP, Kim JK, Yu TX. Improvement of adhesive bonding in aluminium alloys using a laser surface texturing process. *J Mater Process Technol* **63**: 579–584 (1997)

[63] Geiger M, Roth S, Becker W. Influence of laser-produced microstructures on the tribological behavior of ceramics. *Surf Coat Technol* **100-101**: 17–22 (1998)

[64] Geiger M, Popp U, Engel U. Eximer laser micro texturing of cold forging tool surface-influence on tool life. *CIRP Annals* **51**: 231–234 (2002)

[65] Wang X, Kato K, Adachi K, Aizawa K. The effect of laser texturing of SiC surface on the critical load for the transition of water lubrication mode from hydrodynamic to mixed. *Tribol Int* **34**(10): 703–711 (2001)

[66] Kovalchenko A, Ajayi O, Erdemir A, Fenske G, Etsion I. The Effect of laser texturing of steel surfaces and speed-load parameters on the transition of lubrication regime from boundary to hydrodynamic. *Tribol Trans* **47**(2): 299–307 (2004)

[67] Kovalchenko A, Ajayi O, Erdemir A, Fenske G, Etsion I. The effect of laser surface texturing on transitions in lubrication regimes during unidirectional sliding contact. *Tribol Int* **38**(3): 219–225 (2005)

[68] Van Kuilenburg J, Masen M A, Groenendijk M N W, Bana V, van der Heide E. An experimental study on the relation between surface texture and tactile friction. *Tribol Int* **48**: 15–21 (2012)

[69] Van der Heide E, Saenz de Viteri V, Rodringuez-Vidal E, Pagano F, Wadman B, Wiklund D, Matthews D T A, Contreras Fortes J, Zhang S. Steel sheet surfaces with enhanced tactile feel. European Commission Research Programme of the Research Fund for Coal and Steel, RFSR-CT-2011-00022, 2011–2014.

Sheng ZHANG. He received his bachelor degree in mechanical engineering in 2008 from California State University, Fresno, USA, and obtained his Ph.D degree in mechanical engineering at University of Twente, Enschede, the Netherlands. He has recently joined the State Key Laboratory of Tribology in Tsinghua University as a post-doctoral researcher in 2016. His research interests include bio-tribology and surface texture design.

Emile VAN DER HEIDE. He obtained his M.S. and Ph.D degrees in mechanical engineering from University of Twente in 1995 and 2002. His current position is a professor, chair of Skin Tribology, Laboratory for Surface Technology and Tribology, Faculty of Engineering Technology, University of Twente. He has received President's International Fellowship 2016/17 from Chinese Academy of Sciences. His research areas cover the surface engineering, bio-tribology and contact mechanics.